Dynamic recrystallization and microstructure evolution of a powder metallurgy nickel-based superalloy under hot working

Yanhui Liu,[a] Yongquan Ning, Zekun Yao, Yuzhi Li, and Jingli Zhang
School of Materials Science & Engineering, Northwestern Polytechnical University, Xi'an 710072, People's Republic of China

Mingwang Fu
Department of Mechanical Engineering, The Hong Kong Polytechnic University, Hung Hom, Kowloon, Hong Kong

(Received 25 November 2015; accepted 11 May 2016)

The deformation behaviors (flow behavior, power dissipation, dynamic recrystallization, and microstructure evolution) of a typical powder metallurgy nickel-based superalloy were investigated in compression tests at temperatures range of 1020–1140 °C and strain rates range of 0.001–1.0 s^{-1} with the true strains of 0.3, 0.5, and 0.7, respectively. The efficiency of power dissipation can be shown by the power dissipation maps at different true strains. The results showed that true strain had a great effect on the power dissipation. Besides, the deformed microstructures were investigated. The processes of microstructure evolution at different deformation temperatures and strain rates are different. The continuous dynamic recrystallization takes place at the deformation condition of 1080 °C/0.1 s^{-1}. The fine and uniform dynamic recrystallized grains gradually replace the pre-existing grains with the increase of true strain. The discontinuous dynamic recrystallization takes place at the deformation condition of 1110 °C/0.001 s^{-1}. The fine dynamic recrystallized grains grow up and a part of new fine grains appear in the dynamic recrystallized grains because of the periodic dynamic recrystallization.

I. INTRODUCTION

Hot plastic deformation as an important processing method has been widely used for making critical components. This process can not only provide the desired size and shape, but also produce excellent microstructure. The size and shape of component are changed in hot deformation process, which is accompanied by dynamic softening and microstructure evolution.[1–3] Hot plastic deformation as a complex process includes work hardening, dynamic softening and microstructure evolution. All of them are affected by deformation temperature, strain rate, and true strain. And dynamic softening includes dynamic recovery and dynamic recrystallization, which determines the deformed microstructure and performance. Therefore, this is far and away the most important area of hot deformation.

Superalloys have been widely used in manufacturing turbine engine blades or other bearing components working at high temperature because of their good microstructure stability, excellent mechanical properties, good ultimate strength, and creep performance at high temperature.[4–7] With the continuous development of aerospace technology, alloying extent has become increasingly high. Traditional superalloys can no longer satisfy the needs of the development of present aerospace technology. A new type of superalloy was produced by adopting the method of powder metallurgy processing with fine grain, uniform organization, no macro segregation, and high degree of alloying.

FGH4096 superalloy as a kind of powder metallurgy superalloy has been widely applied for manufacturing turbine engine blades or other bearing components at high temperatures.[8,9] With the rapid development of aeronautic and astronautic technology, the turbine inlet temperature is getting higher, which demands higher comprehensive performance for the high temperature components. This kind of powder metallurgy superalloy has a strong application background in aviation and space industry. Therefore, it is significant to research the hot deformation behaviors and microstructure evolution of this superalloy.

However, there is rare research on the whole processes of dynamic recrystallization and microstructure evolution. It is difficult to research the whole process, which is dynamic and continuous. The main aim of the present work is to consider how the microstructure evolution takes place during hot deformation. The deformed microstructures at different true strains were researched, by which to deduce the change rule during the deformation process. The result will significantly benefit the study of microstructure evolution and thus exhibit an important reference value to the future work.

Contributing Editor: Jürgen Eckert
[a]Address all correspondence to this author.
e-mail: liuyanhui36@mail.nwpu.edu.cn
DOI: 10.1557/jmr.2016.204

 © Materials Research Society 2016

https://doi.org/10.1557/jmr.2016.204 Published online by Cambridge University Press

In this work, the hot deformation behavior of powder metallurgy superalloy FGH4096 has been investigated based on the isothermal compression tests conducted at different deformation temperatures, strain rates, and true strains. The relationship between flow stress and true strain was recorded for each deformation temperature and strain rate during hot deformation. The deformed microstructure has been adopted to research the dynamic softening and microstructure evolution. Based on the research results, deformation temperatures and strain rates can be optimized for this powder metallurgy superalloy. These results will provide some theoretical basis for farther experimental research of this powder metallurgy superalloy.

II. EXPERIMENTAL MATERIALS AND PROCEDURES

The investigated material was FGH4096 superalloy prepared with powder metallurgy method produced by hot isostatic press (HIP). Powder particles were procured by argon atomization, and the diameters of powder particles ranged from 80 to 110 μm. The chemical composition of powder particles for producing FGH4096 superalloy used in this present study (wt%) is: 0.03 C, 16.15 Cr, 12.73 Co, 4.02 W, 2.23 Al, 3.71 Ti, balance Ni. The powder particles were encapsulated in a stainless steel capsule, and then produced by HIP (the temperature is about 1100–1150 °C and the press is about 110 MPa for 3 h).

The compression specimens were machined into cylindrical with a height of 12 mm and a diameter of 8 mm from the original bar. In the process of machining, the end surfaces of compression specimens should be ensured perpendicular to the axis of the samples. Besides, to reduce the surface roughness on both end faces of the specimens, the end faces of the specimens should be grinded on a grinding machine.

Isothermal hot compression tests were conducted using a Gleeble-1500D thermo-simulation machine (Dynamic Systems lnc., Troy, New York) in the deformation temperatures range of 1020–1140 °C and in the constant strain rates range of 0.001–1.0 s^{-1}. The true strains are 0.3, 0.5, and 0.7, respectively. All specimens were heated up to the desired temperature at a heating rate of 10 °C/s, and soaked for 300 s at the deformation temperature to obtain a uniform temperature distribution in the entire specimen and gain the uniform microstructure before the hot compression test. In the process of hot deformation, deformation temperature errors were controlled to ±2 °C. The whole processes of heating, heat preservation, and hot deformation were protected by the argon. The load-stroke data obtained in compression were processed to obtain true stress–true strain curves using standard equations. To research the microstructure evolution and the dynamic recrystallization, the specimens after compression tests were sliced along the axial section and the grain structures of the deformed specimens were observed by an Olympus PM3 optical microscope (Olympus Corporation, Tokyo, Japan).

III. RESULTS AND DISCUSSION

A. Initial microstructure of powder metallurgy superalloy

Figure 1 presents the typical microstructure of the as-received powder metallurgy superalloy FGH4096 before hot deformation. The microstructure of this powder metallurgy superalloy is composed of new apparently undeformed powder particles. However, without casting, a great number of previous particle boundaries are still retained. Microscope examination of the specimen reveals cuboidal or cubic γ′ precipitates and carbide particles, mainly at the grain boundaries. And the microstructure reveals a prior particle boundary network by the large primary γ′ precipitates and carbides.

B. Flow stress curves of powder metallurgy superalloy

True stress–true strain curve is a significant way to research the hot deformation behavior, which is used to indicate the intrinsic relationship between work hardening and dynamic softening.[10,11] To study the high-temperature flow behavior of this powder metallurgy superalloy, true stress–true strain curves under different deformation temperatures and strain rates were measured. Typical true stress–true strain curves of this studied powder metallurgy superalloy recorded at various deformation temperatures and strain rates are presented in Fig. 2, which correspond to the deformation temperatures of 1020, 1050, 1080, 1110 and 1140 °C, respectively. As shown in Fig. 2, the flow stress is sensitive to the true strain. It is obvious that the flow stress has different change regularities at different strain scopes. These flow stress curves exhibit a flow softening feature, which is more significant at lower temperatures and higher strain rates. They are composed of three stages: stage I (work hardening stage), stage II (softening stage), and stage III (steady stage). All of the three stages are influenced by combination effect of work hardening and thermally activated softening.[12] In the stage I, the flow stress increases sharply until to a peak stress at a very small true strain. The dislocation density increases because of the dislocation proliferation and the formation of poorly developed subgrain boundaries, leading to the rapid rise of flow stress at the beginning of deformation. Besides, the dynamic recovery proceeds slowly because of the low stacking fault energy. In a word, the dynamic softening

https://doi.org/10.1557/jmr.2016.204 Published online by Cambridge University Press

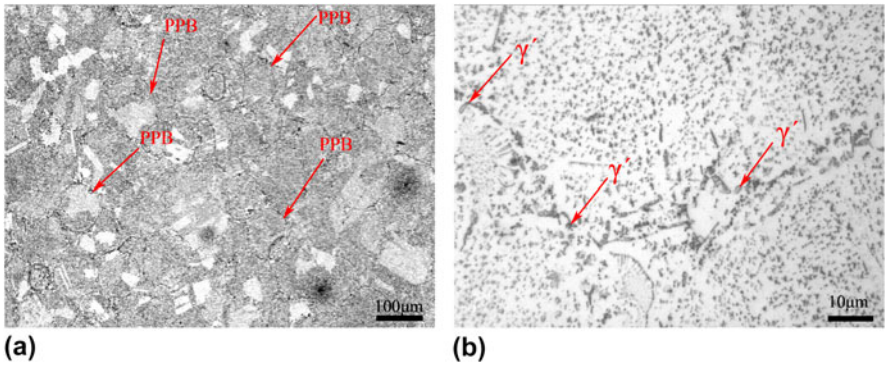


FIG. 1. Typical microstructure of nickel-based powder metallurgy superalloy exhibiting a uniform dispersion of a few undeformed powder particles in a recrystallization-grained matrix: (a) optical micrograph; (b) scanning electron micrograph (SEM) micrograph.

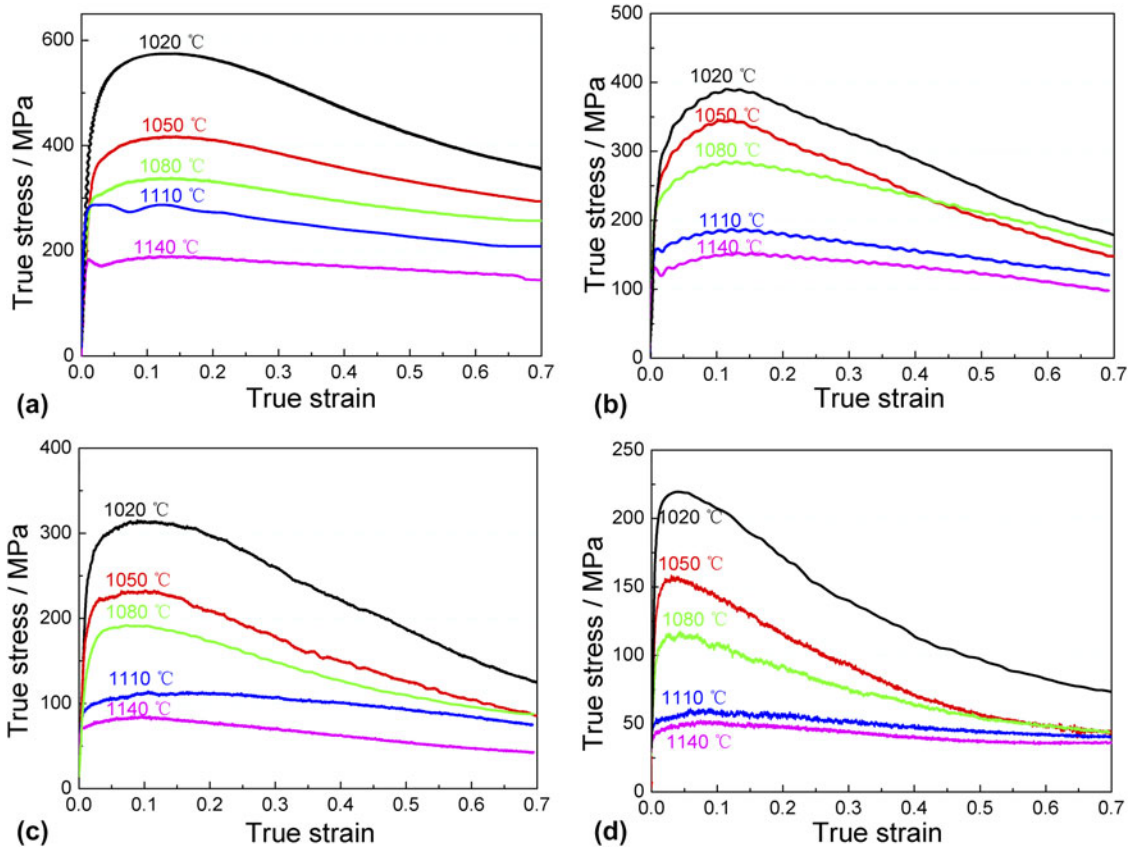


FIG. 2. True stress–strain curves of FGH4096 superalloy hot-compressed at different strain rates: (a) 1.0 s^{-1}; (b) 0.1 s^{-1}; (c) 0.01 s^{-1}; (d) 0.001 s^{-1}.

mechanism almost does not take place in this stage because of the low stacking fault energy, and the effect of work hardening caused by the dislocation multiplication results in the sharp increase of flow stress. In the stage II, the flow stress decreases gradually with the increase of true strain. With the deformation continuous, dislocation density sharply increases and reaches to a critical value. With the rapid proliferation of dislocation, dynamic recrystallization takes place at a high dislocation density once a critical strain (usually less than 0.1) is exceeded. Besides, the stored energy in materials increases because of the dislocation proliferation, meanwhile, nucleation and growth of new grains occur when dislocation densities reach a certain threshold. The effect of dynamic softening plays a leading role at this moment, which is greater than that of work hardening, so the flow stress decreased gradually with the increase of true strain. Finally, in the stage III, the

https://doi.org/10.1557/jmr.2016.204 Published online by Cambridge University Press

flow stress maintains a relatively stable state when the strain reaches a fixed value. In this deformation period, the flow stress keeps steady when the effect of dynamic softening and work hardening reaches a dynamic balance.[13,14]

Besides, as shown in Fig. 2, both deformation temperature and strain rate have a significant effect on the flow stress. The effect can be explained by the terms of dynamic recrystallization and dislocation mechanism. For a constant strain rate, the flow stress decreases with the increase of deformation temperature. The atoms in this powder metallurgy superalloy become more active with the increase of deformation temperature, then the binding force between atoms decreases and more slip systems started. The higher deformation temperature makes dislocations become more active, it means that dislocations can overcome the pinning effect and accomplish the activities such as the climb of edge dislocation and the cross-slip of screw dislocation. Meanwhile both the nucleation rate and growth rate of dynamic recrystallized grain also increase with the increase of deformation temperature, so the softening effect strengthens, leading to the decrease of flow stress.[15] For a constant deformation temperature, the flow stress increases with the increase of strain rate. Because of the shorter deformation time at a higher strain rate, on the one hand, a great number of dislocations pile-up quickly, on the other hand, a shorter time provided for energy accumulation and dynamic recrystallization cannot occur completely. Therefore, it increases the critical shear stress for starting the slip systems during hot deformation, resulting in the increase of flow stress.

C. Effects of strain on the efficiency of power dissipation

Softening mechanism plays a significant role in the process of hot deformation. During hot deformation, the predominant softening mechanisms include dynamic recovery and dynamic recrystallization, which is controlled by activation energy. The efficiency of power dissipation determines the energy distribution, which is significant for dynamic recrystallization and microstructure evolution.

The processing map as a very useful approach has been widely used for investigating the hot plastic deformation.[16–20] It can be used to predict flow behavior, and optimize process parameters for improving deformed microstructure. The dynamic materials model as the basic principle of the processing map assumes that most of the instantaneous power P absorbed by work-piece is dissipated by the dissipater content G and the dissipater co–content J. G is the power dissipated via plastic deformation. J is the work related to metallurgical evolution via different mechanisms such as phase transition, dynamic recovery, and dynamic recrystallization, occurring dynamically to dissipate power. The total power absorbed P can be determined as:

$$P = \sigma\dot{\varepsilon} = \int_0^{\dot{\varepsilon}} \sigma \mathrm{d}\dot{\varepsilon} + \int_0^{\sigma} \dot{\varepsilon}\mathrm{d}\sigma = G + J \quad . \qquad (1)$$

The ratio of $\mathrm{d}J/\mathrm{d}G$ is equivalent to the strain rate sensitivity exponent m. For an ideal linear dissipater, $m = 1$ and $J_{\max} = \sigma\dot{\varepsilon}/2$. By normalizing the instantaneous J with the maximum value, the efficiency of power dissipation η can be defined as:

$$\eta = \frac{J}{J_{\max}} = \frac{2m}{1+m} \quad . \qquad (2)$$

The power dissipation map is obtained by plotting isoefficiency contour map of the parameter η.

The values of η at different deformation temperatures and strain rates can be got based on Eq. (2). The power dissipation maps can be obtained by plotting isoefficiency contour map of the parameter η. Figure 3 shows the variation in the efficiency of power dissipation with the change of true strain from 0.1 to 0.7. In these maps, the numbers represent the efficiency of power dissipation (η) as percentage.

D. Dynamic recrystallization and microstructure evolution

Based on Fig. 3, the efficiency of power dissipation is significantly affected by deformation temperature, strain rate, and true strain. Three special domains (A: 1020 °C/1.0 s^{-1}, B: 1080 °C/0.1 s^{-1}, C: 1110 °C/0.001 s^{-1}) in these maps were investigated. The change of power dissipation and microstructure evolution at different true strains were studied.

The variations in the efficiency of power dissipation with true strains at the temperature of 1020 °C and the strain rate of 1.0 s^{-1} are shown in Fig. 4. The values of power dissipation continuously increase with the increase of true strain. When the true strain is less than 0.5, the values of power dissipation significantly increase; while the true strain is larger than 0.5, the values of power dissipation slowly increase. The values of power dissipation reflect the energy which relates to metallurgical evolution via different mechanisms such as phase transition, dynamic recovery, and dynamic recrystallization. At this low temperature and high strain rate, dynamic recrystallization is not easy to take place. A great number of dislocations constantly generate in the process of hot deformation. The deformation energy increases with the increase of true strain, which contribute to dislocation multiplication and stacking. Dynamic recovery and dynamic recrystallization only take

https://doi.org/10.1557/jmr.2016.204 Published online by Cambridge University Press

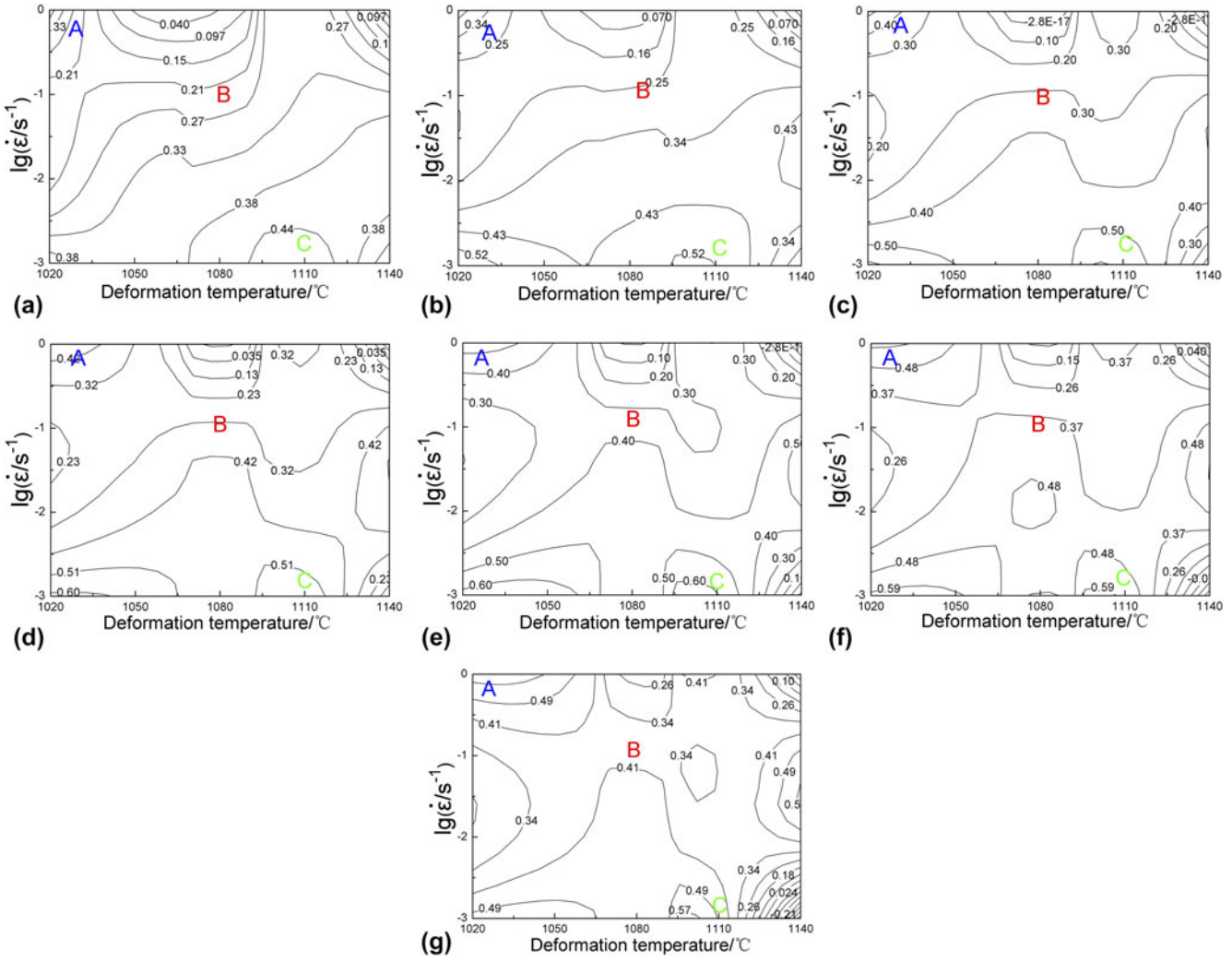


FIG. 3. Power dissipation maps of FGH4096 superalloy at the true strains of 0.1 (a) to 0.7 (g). The contour numbers represent the efficiency of power dissipation (η).

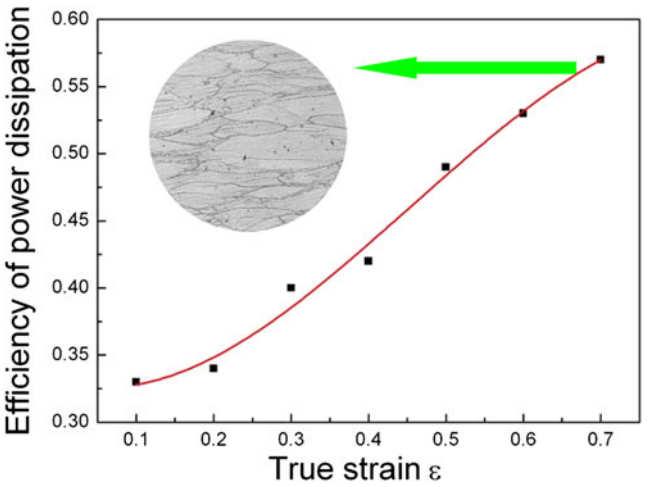


FIG. 4. Variation in the efficiency of power dissipation with true strains at the temperature of 1020 °C and at the strain rate of 1.0 s^{-1}.

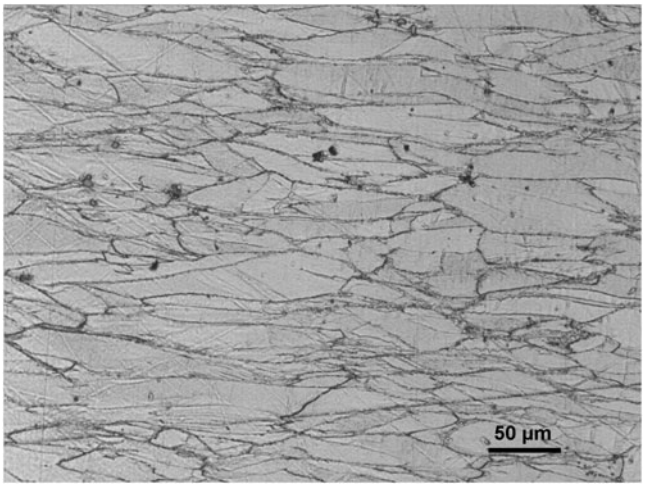


FIG. 5. Typical deformed microstructure of FGH4096 superalloy at deformation condition of 1020 °C/1.0 s^{-1} and true strain of 0.7.

https://doi.org/10.1557/jmr.2016.204 Published online by Cambridge University Press

place when the deformation energy reaches a critical value.

The typical deformed microstructure at deformation condition of 1020 °C/1.0 s^{-1} and true strain of 0.7 is shown in Fig. 5. In the microstructure, the pre-existing grains are clearly visible, and they are elongated in the deformation direction. The deformation energy that the microstructure got cannot meet the needs of hot deformation activation energy, and dynamic recrystallization is not easy to take place, because of the low deformation temperature and the high strain rate. A very small amount of fine dynamic recrystallized grains distribute along the pre-existing grain boundaries especially at trigonal grain-boundary as shown in Fig. 5.

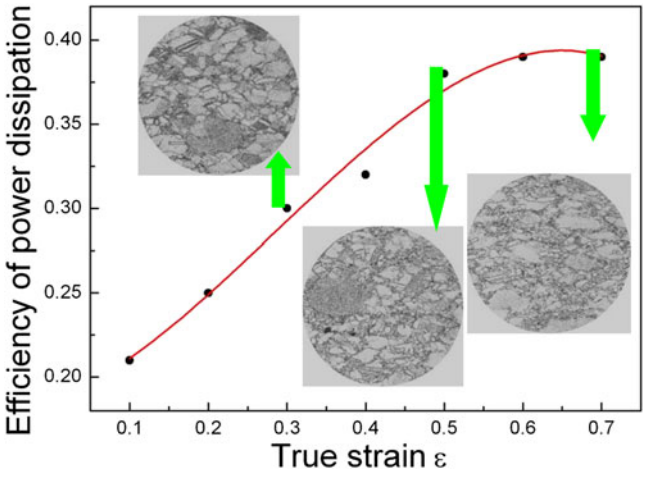


FIG. 6. Variation in the efficiency of power dissipation with true strains at the temperature of 1080 °C and at the strain rate of 0.1 s^{-1}.

The variations in the efficiency of power dissipation with true strains at the temperature of 1080 °C and the strain rate of 0.1 s^{-1} are shown in Fig. 6. The values of power dissipation changed with the increase of true strain. When the true strain is less than 0.6, the values of power dissipation significantly increase; while the true strain is larger than 0.6, the values of power dissipation mainly keep invariant. At the beginning of hot deformation, dynamic recrystallization cannot take place because of low energy. A great number of dislocations are constantly generated in the process of hot deformation, which leads to the increase of deformation energy. When the strain reached a critical value, recrystallization takes place in abundant grains, so the values of power dissipation mainly keep invariant.

Typical deformed microstructures at the deformation condition of 1080 °C/0.1 s^{-1} and different true strains are shown in Fig. 7. As these figures shown, the microstructures have a great change with the increase of true strain, which has the inner link with the power dissipation. At true strain of $\varepsilon = 0.3$, the power dissipation is about 30%, which indicates that the energy for dynamic recrystallization is not enough and cannot meet the needs of hot deformation activation

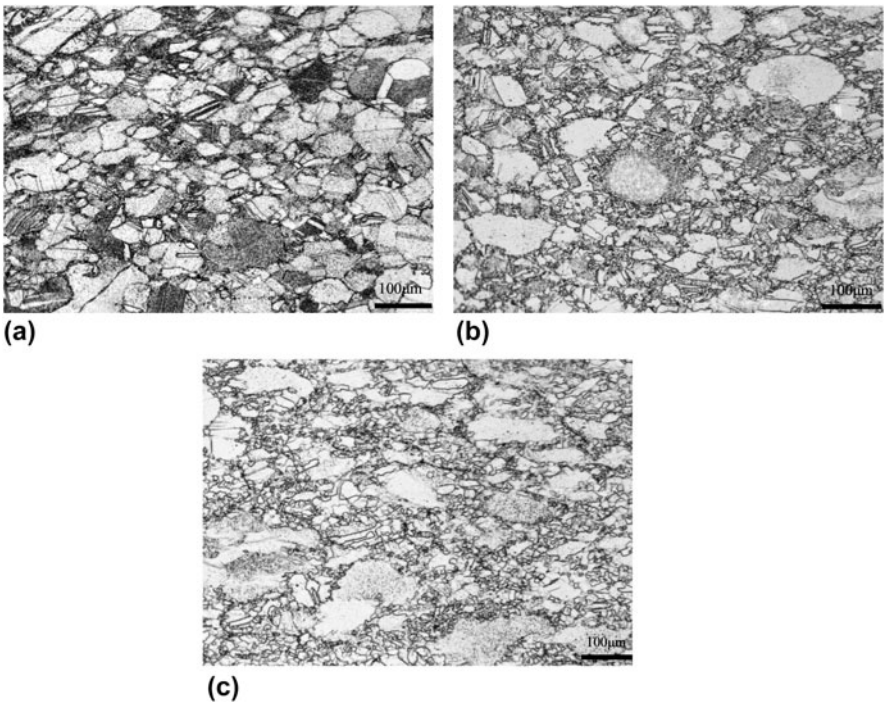


FIG. 7. Typical deformed microstructures of FGH4096 superalloy at deformation condition of 1080 °C/0.1 s^{-1} and different true strains: (a) 0.3; (b) 0.5; (c) 0.7.

https://doi.org/10.1557/jmr.2016.204 Published online by Cambridge University Press

energy, so dynamic recrystallization does not take place almost. The boundaries of pre-existing grains in Fig. 7(a) are frequently serrated and a few submicrometer-scale grains are observed near pre-existing grain boundaries, especially at triple junctions. At a true strain of $\varepsilon = 0.5$, the power dissipation increases to 38%. The deformation energy for dynamic recrystallization constantly accumulated with the increase of true strain, which is beneficial to the occurrence of dynamic recrystallization. The deformation structure is characterized by pancake-shaped original grains that are decorated with chains of ultrafine grains [Fig. 7(b)]. The formation of new grains takes place along the original grain boundaries, resulting in the development of the so-called necklace microstructure.[21] Besides, the smaller the original grain, the more new grains take place along the boundaries. Because the moving dislocations are piled up in the vicinity of needle-shaped γ' phases during the hot forming, the element Nb can be sucked to the surroundings of the dislocations, which can offer a fast path for the diffusion of Nb.[22] However, the existence of γ' phases in the studied superalloy can increase the rate of dislocation generation and promote the nucleation of dynamic recrystallization (DRX). Simultaneously, the γ' phase has a strong pinning effect on the grain boundary to inhabit the growth of recrystallized grain. At true strains of $\varepsilon = 0.6$ and $\varepsilon = 0.7$, the power dissiue. It indicates that the continuous dynamic recrystallization takes place at these deformation parameters. With the continuous hot deformation, the value of the power dissipation increases to 39%, which is beneficial to the dynamic recrystallization. At this stage of deformation, more deformation energy is used for dynamic recrystallization, more grains take place dynamic recrystallization and more new grains take place along the pre-existing grain boundaries. Based on the deformation microstructure [Fig. 7(c)], almost every original grain is surrounded by new small grains. It can be seen that the dynamic recrystallization results in significant grain refinement. The fraction of new recrystallized grains amount to ~0.6, and a part of pre-existing coarse grains are replaced by the recrystallized grains. While the dynamic recrystallization has not finished completely, some unrecrystallized, and hence work-hardened, coarse grains, which are portions of pre-existing grains, are highly elongated crosswise to the compression axis.

Based on Fig. 3, the peak efficiency of power dissipation corresponding to the domain of 1110 °C/0.001 s^{-1}, and the efficiency of power dissipation is significantly affected by the true strain. The variations in the efficiency of power dissipation with true strains at the temperature of 1110 °C and the strain rate of 0.001 s^{-1} are shown in Fig. 8. The values of power dissipation significantly fluctuated with the increase of true strain, and a multiple peak behavior can be noticed. Power dissipation rapidly increases with the

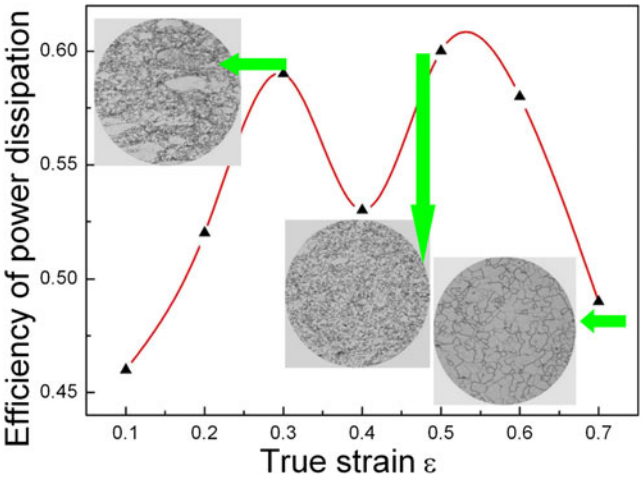


FIG. 8. Variation in the efficiency of power dissipation with true strains at the temperature of 1110 °C and at the strain rate of 0.001 s^{-1}.

increase of true strain in the true strain range of 0.1–0.3, on the contrary, it significantly decreases in the strain range of 0.3–0.4. In the following deformation period, the power dissipation first increases and then gradually decreases with the increase of true strain. There are two peak points corresponding to 0.3 and 0.53. This phenomenon may be attributed to the occurrence of several independent cycles of dynamic recrystallization.

The typical deformed microstructure at deformation condition of 1110 °C/0.001 s^{-1} and different true strains are shown in Fig. 9. At true strain of $\varepsilon = 0.3$, dynamic recrystallization takes place at a low strain because of the high deformation temperature and low strain rate. A part of small original grains are replaced by the fine dynamic recrystallized grains, the remaining great number of dynamic recrystallized grains generated around the original grains [Fig. 9(a)]. At true strain of $\varepsilon = 0.5$, the complete dynamic recrystallization almost has finished. So the original grains are completely replaced by the fine and uniform recrystallized grains [Fig. 9(b)]. Spontaneous nucleation takes place at this deformation parameter, which assured the complete dynamic recrystallization. At deformation condition of 1110 °C/0.001 s^{-1}, fine and homogenous microstructure can be achieved at the true strain of 0.5. After this process of dynamic recrystallization finished, the new grains can be found on the recrystallization grains [Fig. 9(c)]. It indicates that the periodic dynamic recrystallization take place at this deformation parameter. This periodic dynamic recrystallization phenomenon corresponds to the change of power dissipation. Besides, because the dynamic recrystallized grains stayed at a high temperature for a long time, the fine grains got in the first dynamic recrystallization significantly grow up.

https://doi.org/10.1557/jmr.2016.204 Published online by Cambridge University Press

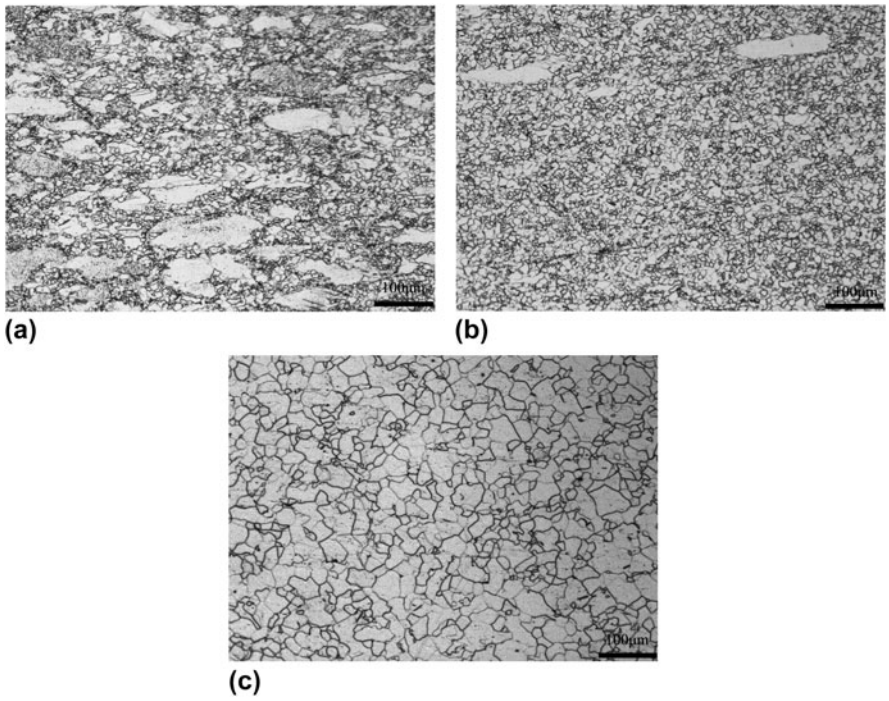


FIG. 9. Typical deformed microstructure of FGH4096 superalloy at deformation condition of 1110 °C/0.001 s^{-1} and different true strains: (a) 0.3; (b) 0.5; (c) 0.7.

IV. CONCLUSIONS

The deformation behaviors (flow behavior, power dissipation, dynamic recrystallization, and microstructure evolution) of the powder metallurgy nickel-based superalloy were investigated in compression tests at temperatures range of 1020–1140 °C and strain rates range of 0.001–1.0 s^{-1}. The main conclusions can be summarized as follows:

(1) The flow stress is the external expression of the combined result of work hardening and dynamic softening. All the stress–strain curves of this nickel-based superalloy are composed of three stages: stage I (work hardening stage), stage II (softening stage), and stage III (steady stage).

(2) The efficiency of power dissipation increases significantly with the increase of true strain at the deformation condition of 1020 °C/1.0 s^{-1}; while it increases first and keeps constant then with the increase of true strain at deformation condition of 1080 °C/0.1 s^{-1}; and the peak value of power dissipation presents at the deformation condition of 1110 °C/0.001 s^{-1}.

(3) The pre-existing grains, clearly visible, are elongated in the deformation direction at the deformation condition of 1020 °C/1.0 s^{-1}. A very small amount of fine dynamic recrystallized grains distribute along the pre-existing grain boundaries especially at trigonal grain-boundary. The continuous dynamic recrystallization takes place at the deformation condition of 1080 °C/0.1 s^{-1}. The fine and uniform dynamic recrystallization grains gradually replace the pre-existing grains with the increase of strain. The discontinuous dynamic recrystallization takes place at deformation condition of 1110 °C/0.001 s^{-1}. The fine dynamic recrystallization grains grow up and a part of new fine grains appear in the dynamic recrystallization grains because of the periodic dynamic recrystallization.

ACKNOWLEDGMENTS

This work was financially supported by the national natural science foundation of China (Grant No. 51101119 and Grant No. 51175431), the postdoctoral science foundation of China (Grant No. 2015M570851), and the fundamental research funds for the central universities (Grant No. 3102016ZY012). Also, we would like to thank the funding support by the Hong Kong scholar program (Grant No. XJ2014047 and G-YZ68).

REFERENCES

1. F.L. Jiang, H. Zhang, L.X. Li, and J.H. Chen: The kinetics of dynamic and static softening during multistage hot deformation of 7150 aluminum alloy. *Mater. Sci. Eng., A* **552**, 269–275 (2012).
2. X.M. Chen, Y.C. Lin, M.S. Chen, H.B. Li, D.X. Wen, J.L. Zhang, and M. He: Microstructural evolution of a nickel-based superalloy during hot deformation. *Mater. Des.* **77**, 41–49 (2015).
3. Y.C. Lin, L.T. Li, Y.X. Fu, and Y.Q. Jiang: Hot compressive deformation behavior of 7075 Al alloy under elevated temperature. *J. Mater. Sci.* **47**(3), 1306–1318 (2012).

https://doi.org/10.1557/jmr.2016.204 Published online by Cambridge University Press

4. L. Tian, Q. Ao, and S.L. Li: Effect of austenitic state on microstructure and mechanical properties of martensite/bainite steel. *J. Mater. Res.* **29**(7), 887–895 (2014).
5. Z.L. Li, Q.Y. Xu, and B.C. Liu: Microstructure simulation on recrystallization of an as-cast nickel based single crystal superalloy. *Comput. Mater. Sci.* **107**, 122–133 (2015).
6. Y.Z. Liu, X.B. Hu, S.J. Zheng, Y.L. Zhu, H. Wei, and X.L. Ma: Microstructural evolution of the interface between NiCrAlY coating and superalloy during isothermal oxidation. *Mater. Des.* **80**, 63–69 (2015).
7. W. Sun, X.Z. Qin, J.T. Guo, L.H. Lou, and L.Z. Zhou: Thermal stability of primary MC carbide and its influence on the performance of cast Ni-base superalloys. *Mater. Des.* **69**, 81–88 (2015).
8. Q. Bai, J. Lin, J. Jiang, T.A. Dean, J. Zou, and G. Tian: A study of direct forging process for powder superalloys. *Mater. Sci. Eng., A* **621**, 68–75 (2015).
9. L.T. Chang, W.R. Sun, Y.Y. Cui, F.Q. Zhang, and R. Yang: Effect of heat treatment on microstructure and mechanical properties of the hot-isostatic-pressed Inconel 718 powder compact. *J. Alloys Compd.* **590**, 227–232 (2014).
10. M.H. Wang, Y.F. Li, W.H. Wang, J. Zhou, and A. Chiba: Quantitative analysis of work hardening and dynamic softening behavior of low carbon alloy steel based on the flow stress. *Mater. Des.* **45**, 384–392 (2013).
11. L.X. Li, B. Ye, S. Liu, S.D. Hu, and B. Li: Inverse analysis of the stress–strain curve to determine the materials models of work hardening and dynamic recovery. *Mater. Sci. Eng., A* **636**, 243–248 (2015).
12. K. Wu, G.Q. Liu, B.F. Hu, F. Li, Y.W. Zhang, Y. Tao, and J.T. Liu: Hot compressive deformation behavior of a new hot isostatically pressed Ni–Cr–Co based powder metallurgy superalloy. *Mater. Des.* **32**, 1872–1879 (2011).
13. D.F. Li, Q.M. Guo, S.L. Guo, H.J. Peng, and Z.G. Wu: The microstructure evolution and nucleation mechanisms of dynamic recrystallization in hot-deformed Inconel 625 superalloy. *Mater. Des.* **32**, 696–705 (2011).
14. L.H. Rettberg and T.M. Pollock: Localized recrystallization during creep in nickel-based superalloys GTD444 and René N5. *Acta Mater.* **73**, 287–297 (2014).
15. Z.W. Cai, F.X. Chen, and J.Q. Guo: Constitutive model for elevated temperature flow stress of AZ41M magnesium alloy considering the compensation of strain. *J. Alloys Compd.* **648**, 215–222 (2015).
16. Y.H. Liu, Y.Q. Ning, Z.K. Yao, and M.W. Fu: Hot deformation behavior of the 1.15C–4.00Cr–3.00V–6.00W–5.00Mo powder metallurgy high speed steel. *Mater. Des.* **54**, 854–863 (2014).
17. H. Jiang, J.X. Dong, M.C. Zhang, L. Zheng, and Z.H. Yao: Hot deformation characteristics of alloy 617B nickel-based superalloy: A study using processing map. *J. Alloys Compd.* **647**, 338–350 (2015).
18. Y. Wang, Q.L. Pan, Y.F. Song, C. Li, and Z.F. Li: Hot deformation and processing maps of X-750 nickel-based superalloy. *Mater. Des.* **51**, 154–160 (2013).
19. Y.H. Liu, Y.Q. Ning, Y. Nan, H.Q. Liang, Y.Z. Li, and Z.L. Zhao: Characterization of hot deformation behavior and processing map of FGH4096-GH4133B dual alloys. *J. Alloys Compd.* **633**, 505–515 (2015).
20. X. Shang, J. Zhou, X. Wang, and Y. Luo: Optimizing and identifying the process parameters of AZ31 magnesium alloy in hot compression on the base of processing maps. *J. Alloys Compd.* **629**, 155–161 (2015).
21. Y.Q. Ning, C. Zhou, H.Q. Liang, and M.W. Fu: Abnormal flow behavior and necklace microstructure of powder metallurgy superalloys with previous particle boundaries (PPBs). *Mater. Sci. Eng., A* **652**, 84–91 (2016).
22. H.Y. Zhang, S.H. Zhang, M. Cheng, and Z.X. Li: Deformation characteristics of δ phase in the delta-processed Inconel 718 alloy. *Mater. Charact.* **61**, 49–53 (2010).

https://doi.org/10.1557/jmr.2016.204 Published online by Cambridge University Press